RSC Advances

ROYAL SOCIETY OF CHEMISTRY

www.rsc.org/advances

Journal Name

ARTICLE

Synthesis and thermal degradation property study of N-vinylpyrrolidone and acrylamide copolymer

Lili Xu[a], Jing Zheng[b,*], Lixia Che[b], Xiaorong Wu[c], Pengdao Chen[c], Liyu Zhang[c], Qiaoman Hu[c] and Guangsu Huang[*]

A series of acrylamide (AM) copolymers with various N–Vinylpyrrolidone (NVP) contents were prepared by free radical solution polymerization. The chemical structures of polyacrylamide (PAM) and copolymers were analyzed by Fourier Transform Infrared Spectrometer (FTIR) and H NMR. Systematic investigations had been carried out to reveal the role of NVP in copolymer thermal degradation by using a variety of techniques--differential scanning calorimetry (DSC), thermogravimetric analysis (TGA), thermogravimetric analysis coupled Fourier Transform Infrared Spectroscopy (TGA-FTIR). The DSC measurement showed an increase of 18 $^{\circ}$C in glass transition temperature (T_g) for copolymer, meaning better thermal stability at 10% NVP content. TGA-FTIR analysis revealed that in copolymer, low temperature pyrolysis products, such as ammonia and amide, were slowed down until NVP cleaved at about 400 $^{\circ}$C. Furthermore, nitriles which derived from imide or isolated amide breakdown, were only detected in copolymer over 350 $^{\circ}$C, verifying that amide or imide groups in copolymer were also protected by NVP from another point of view. These results also revealed that NVP formed hydrogen bond with amide group and promoted the remote side group or inter-molecule crosslinking under heating.

Introduction

Polyacrylamide, along with poly(N-vinylpyrrolidone), performs favorable physical or chemical stability in biological body, widely utilized as soft tissue filler in aesthetic and plastic surgery, [1] drug and cell carriers [2] in clinical medicine. Furthermore, polyacrylamide has also become very attractive material for gel electrophoresis, used for DNA adducts detection, [3,4] DNA sequencing, [5] separation of proteins in native biomacromolecule, [6] amino acids, [7] lipids, nucleotides, sugars.

In recent years, there has also been an increasing interest in polyacrylamide and poly(N-vinylpyrrolidone) as proton conducting polymeric electrolytes matrix [8,9] in various electrochemical devices working in a wide temperature range, such as electronical condenser, electrochromic displays, electroplate and electrolytes solution. Polyacrylamide has also become very attractive materials for a variety of applications, including even as phantom for radiofrequency ablation, [11] acoustic coupling medium. [12]

N-vinylpyrrolidone, as an effective co-monomer in thermal stability and amphipathy, was introduced into acrylamide copolymer in many fields, such as water reducer, sewage treatment agent and oil-displacing agent. [13] One of the most critical limiting factors of the application of polymeric materials is their limited thermal stability. However, in spite of the growing interest in acrylamide copolymer and their high-

temperature applications, only sporadic reports can be found on their thermal degradation or pyrolysis products analysis, and according to the best of our knowledge, systematic detailed investigations on the thermal degradation of poly(acrylamide-vinylpyrrolidone) have not been reported yet. Most of the publications displayed thermal degradation behavior of polyacrylamide and poly(2-vinyl-pyrrolidone),[10,14,15] or compositing with polymer, [10,16~21] metal [22~25] or ceramic materials. [26~31]

Some of these studies also reported on certain thermal data, for example, poly(vinyl-pyrrolidone), PVP, with a T_g of 175 $^{\circ}$C (MW=400,000), performed a major decomposition at 480 $^{\circ}$C, and though its degradation mechanisms differed radically from each other in previous works, pyrrolydone pendant group removal at the first stage is gernally accepted. [10,15,19]

However, the effect of N-vinylpyrrolidone on thermal stability of polyacrylamide has not been revealed at all yet. Typically, polyacrylamide performs two main thermal degradation at about 300 $^{\circ}$C and 400 $^{\circ}$C, respectively. The thermal degradation of polyacrylamide induces formation of many pyrolysis products at around 450 $^{\circ}$C, such as amides, imides, nitriles, ketones (aldehyde) and acrylamide oligomers. [32]

It is also found that the degradation of acrylamide obeys the Arrhenius kinetics and the corresponding thermal degradation activation energy is about 140kcal/mol. Herein, we report on our findings obtained in the course of a series of detailed and systematic investigations on the thermal stability and

degradation process of poly(acrylamide-vinylpyrrolidone). In order to reveal the effect of N-vinylpyrrolidone pendant group on thermal stability and pyrolysis products, calorimetric and thermogravimetric studies were applied in conjunction with online Fourier Transform Infrared Spectroscopy (TG-FTIR) to identify and analyze the pyrolysis products.

Experimental

Materials

The monomer acrylamide (AM) (Chengdu, China) was recrystallized in chloroform and N-vinylpyrrolidone (NVP) (Shanghai, China) refined by decompression distillation. The solvent ethanol, acetone (Chengdu, China) was dehydrated by distillation previously. The initiator tetramethylethylenediamine (TMEDA) (Chengdu, China), potassium persulfate (KPS) (Chengdu, China) and 2,2'-azobis[2-methylpropionamidine] dihydrochloride (AAPH) (Chengdu, China) were all dissolved in deionized water at a concentration of 2 mg/mL.

Preparation of specimens

Acrylamide (AM), along with corresponding amount of N-vinylpyrrolidone (NVP) was added into a three-necked flask with a thermometer, a stirring rod and a nitrogen gas conduit to construct oxygen-free conditions. After about 15 minutes below AM polymerizing temperature, AAPH, TMEDA and KPS solution were added into the mixture [13]. Gelation occurred in about 30 minutes since the addition of initiator, and nitrogen gas was cut off and the whole reactor was sealed. After 24 h, the product was precipitated into acetone, and then extracted in acetone before ethanol to remove residual monomer, oligomer and NVP homopolymer. After extracting, the samples were dried at $40^{o}C$ in a vacuum oven for 3 days and then stored in desiccator at ambient temperature, as seen in Scheme 1.

Specimens with approximate molecule weight were obtained by regulating the amount of initiator in polymerization. Molecule weight of all the specimens was evaluated through intrinsic viscosity with Ubbelohde viscometer according to GB 12005.10-1992.

The NVP/AM ratio of the specimens was 0, 1%, 5%, 10%, 15%, respectively. Hereinafter, the corresponding specimens were named as PAM, P(AM-NVP-1%), P(AM-NVP-5%), P(AM-NVP-10%) and P(AM-NVP-15%).

Characterization

FTIR. FTIR analysis of the specimens was conducted with a Nicolet-560 infrared spectrometer (USA) using a potassium bromide (KBr) pellet. FTIR spectra were recorded in the spectral range of 4000–400 cm^{-1} with a 2 cm-1 resolution and 32 scans.

H NMR. H NMR spectra was recorded on a spectrometer (Varian INOVA-400) at 25 ^{o}C using D_2O as the solvent and HDO as the external standard.

DSC. Differential scanning calorimetry (DSC) was performed with a Q200 DSC calorimeter (TA Instruments, American) in Al crucibles under nitrogen flow. The samples (ca. 3~4 mg) were first heated from 40 ^{o}C to 230 ^{o}C, then cooled to $100^{o}C$ and again heated to $300^{o}C$ in nitrogen at a rate of $20^{o}C/min$. The reported T_g values were determined in the second scans.

TGA-FTIR. Thermogravimetric analysis coupled with Fourier transform infrared spectroscopy, TGA-FTIR, was performed via a Perkin-Elmer thermogravimetric analyzer (METTLER TOLEDO) interfaced to a Nicolet IS 10 infrared spectrometer

under a dry nitrogen atmosphere. The samples (ca. 20~25 mg) were heated from $50^{o}C$ to $700^{o}C$ at a rate of $10^{o}C/min$ in a 70uL alumina ceramic sample holder. The nitrogen flow carried evolved gas into the cell of infrared spectrometer through a capillary tube under macro-program control. IR spectra were recorded in the spectral range of 4000–650 cm^{-1} with a 2 cm^{-1} resolution and 32 scans.

Results and discussion

FTIR Spectra of PAM and copolymer

Fig.1 showed the FTIR spectrum of PAM and copolymer. v_{max}/cm^{-1} 3420(NH stretch), 2924(sym CH_2 stretch, chain), 1680(conj.CO in acrylamide), 1630(NH blend in acrylamide or conj.CO in NVP), 1492(CN scissor, ring [33]), 1454(CH_2 scissor), 1112(CN stretch [34]).

As was seen, the peak at 1680cm^{-1} disappeared with increasing NVP content, indicating amide Ⅰ band shifted to lower wave number, even coincided with amide Ⅱ band. Moreover, sharp peak at 1454 cm^{-1} shrank and a weak peak at 1492 cm^{-1} appeared in copolymer, proving that NVP was successfully introduced.

H NMR study of PAM and copolymer

The H NMR spectrums of PAM and copolymer (PAM-NVP-15% as a template) were shown in Fig.2, and a small amount of residual ethanol was also detected, whose peaks were in accordance with water peak. δ_H (400MHz; D_2O; HDO), 4.79 (1H, s, HDO), 1.17 (3 H, t, $-CH_3$ in ethanol), 3.64 (2 H, q, $-CH_2-$ in ethanol), 1.70 (2 H_b, d, $-CH_2-$ of PAM backbone), 2.2 (1 H_a, d, -CH- of PAM head-to-end connection backbone), 2.33 (1 H_c, s, -CH- of PAM head-to-head connection backbone), 3.35 (1 H_d, m, -CH- of PAM backbone adjacent to initiator). For copolymer, 1.65 (2 H_i, m, $-CH_2-$ of copolymer backbone), 2.0 (2 H_f, s, $-CH_2-$ of pyrrolidone ring), 2.19 (2 H_e and 1 H_a, m, $-CH_2-$ of pyrrolidone ring and -CH- of PAM), 2.34 (1 H_c, s, -CH- of PAM head-to-head connection backbone), 3.27 (2 H_g, s, $-CH_2N-$ in pyrrolidone ring), 3.89 (1 H_j, m, -CH- of backbone connected to pyrrolidone in head-to-end connection), 4.02 (1 H_h, m, -CH- of backbone connected to pyrrolidone in head-to-head connection). According to the area of characteristic peak, the conversions of NVP were 82.4%.

Combining the IR spectrum and H NMR spectra of copolymer, we can conclude that the NVP were successfully introduced into the PAM.

Intrinsic viscosity measurement

Molecule weight (MW) of all the specimens was valued in intrinsic viscosity. The intrinsic viscosity of specimens selected in the paper was listed in table 1. As is seen, the eventual intrinsic viscosity was at around 1000 mL g^{-1}, at an equal MW level of about 4500 kg mol^{-1}.

DSC study of PAM and copolymer

In order to better understand NVP restriction on PAM molecular movement at elevated temperature, a series of NVP contained copolymer was evaluated by DSC in glass transition temperature (T_g). Fig.3 showed the DSC curves of PAM and copolymer with different NVP content. The glass transition temperature increased with extending NVP content, from 194 ^{o}C for PAM to 212 ^{o}C for PAM-NVP-10%, chiefly because appropriate amount of NVP content was uniformly dispersed in

RSC Advances Accepted Manuscript

copolymer, in which large steric hindrance of five-membered pyrrolidone ring stiffened the copolymer backbone, so as to enhance its T_g. When NVP content increased to a certain proportion, the T_g started to decrease. As is seen in PAM-NVP-15%, it could be interpreted that NVP got together and tremendously enlarged its free volume, where the adjacent segment could move freely. As a result, the whole molecule flexibility increased and thus T_g decreased.

It is supposed that some special interaction between NVP and PAM enhance the thermal stability of copolymer. Next, TGA-FTIR coupling technique is adopted to further study how NVP plays its role in PAM heat resistance and thermal degradation.

TGA

PAM, PAM-NVP-10%, PAM-NVP-15% were further studied via TGA, as was seen in Fig.4. PAM-NVP-15% performed the worst, especially below 350°C, which was coincident with the free volume presumption previously proposed in DSC analysis, as was listed in table 2. For the sake of comparison, the second stage of copolymer was divided into two subordinate ones at the first maximum in corresponding DTG curve region.

PAM-NVP-10%, possessing the highest T_g and the best performance in TGA, was selected as a template to compare with PAM in thermal degradation. Hereinafter, PAM-NVP-10% was called copolymer in short, unless specially stated.

A little higher mass retention for copolymer was detected in the whole temperature range, especially from 200°C to 500°C, indicating better heat resistance in lower temperature range. Both curves of PAM and copolymer showed a 12% loss as soon as heating was started, during which the volatilization of moisture and residual solvent such as ethanol, was essentially completed at about 200°C. While for PAM, carbon dioxide was also detected below 200°C. As the temperature elevated further, degradation of the polymers began. DTG thermograms (Fig.5) clearly showed that degradation of copolymer was suppressed at about 300°C. While the thermal degradation of copolymer was much more complex, because more subordinate degradation regions at about 310°C, 360°C and 425°C emerged near the maximum rate of weight loss at 400°C. At about 570°C a plateau was observed in the TG curve, as *dw/dt* was zero.

Gas Evolution Studies

Compared with PAM, major degradation of side chain at the second stage was obviously suppressed. The maximum degradation temperature of copolymer was at about 400°C, lower than reported 480°C, the only maximum degradation temperature of pure PVP. These differences implied that the pyrolysis of copolymer was not simply superposition of two copolymer compositions, but interaction with each other under heating. To further demonstrate the special role NVP played in copolymer degradation, the evolved gas was studied by TGA-FTIR analysis.

During TGA-FTIR experiments, spectral data are repeatedly collected and then processed to build up a Gram-Schmidt reconstruction (Fig.6), each point of which corresponds to the total IR absorbance of the evolved components in the range of 4000-650 cm⁻¹, i.e., the Gram-Schmidt plot is the result of averaging all FTIR peak intensities over the entire spectral range [35]. Thus, the total absorbance intensity of each weight loss is function of the concentration of evolved gases and their pyrolysis rate.

The Gram-Schmidt in the TGA-FTIR showed that both sustained three main pyrolysis stages after 15min. However, the copolymer possessed a slighter pyrolysis at the first stage, indicating that NVP suppressed the PAM side chain degradation [36] at lower temperature. A sharp absorption peak was detected at about 30min (350°C) for copolymer, which mainly comprised of carbon dioxide and aldehyde (ketones) dramatic increase at this stage (seen in Fig.7b). Gram-Schmidt was incompletely in accordance with DTG curve, in general the following two reasons accounted: first, not all evolved gas had an IR absorbance; Second, different gases presented variable infrared activity.

To qualitatively study the evolved gases, the best hits on the library search program were confirmed as ammonia, carbon dioxide, aldehydes (ketone), imide and amide for both. Next, all absorption peaks detected were drawn out and assigned to potential pyrolysis products, in which pyrrolidone and nitriles were figured out exclusively for copolymer. The real-time tracking infrared spectrums and intensity of divided pyrolysis component was displayed in Fig.7 and Fig.8.

The peak at 961 cm⁻¹ was attributed to ammonia, the peak at 1660 cm⁻¹ and 1626 cm⁻¹ was attributed to conjugated C=O and unsaturated bond, respectively. The peak at 1660 cm⁻¹ was also a combined mode with the contribution of C=O and C-N stretch [37] in pyrrolidone, the peak at 1702 cm⁻¹ was attributed to C=O of cyclic imide, the peak at 1743 cm⁻¹ was attributed to C=O of aldehydes (ketone), the peaks at 2250 cm⁻¹ and 2280 cm⁻¹ were attributed to nitriles, the peak at 2365 cm⁻¹ was attributed to carbon dioxide.

Ammonia derived from imidization between amide groups, carbon dioxide from carboxyl group degradation, pyrolysis of imide or original carboxyl group degradation at the presence of water for PAM; aldehydes (ketone) and imide mainly from initial backbone breakdown after imidization or amide cleavage at the presence of water; imide, mainly glutarimide [36,38] and ramification from the main chain breakdown. Pyrrolidone mainly came from NVP side group splitting at about 400 °C, which was similar to NVP homopolymer degradation. As is reported, the nitriles mainly derived from imide group breakdown as carbon dioxide emitting or isolated amide group dehydration [38].

For PAM, carbon dioxide was slowly released at the beginning, followed by ammonia rapid liberation, and then carbon dioxide main degradation, followed by imide. For copolymer, ammonia primary emitting started a little later than PAM, followed by carbon dioxide major release, and then imide accompanied by aldehydes (ketone), pyrrolidone and amide.

Combining Gram-Schmidt curves with pyrolysis products, the degradation process was then focused on exclusive pyrolysis products and the maximum thermal degradation at about 400 °C in DTG curve.

Nitriles Analysis

It is reported that PAM pyrolysis products contain nitriles, [40] but we did not detect the characteristic C≡N peak (Fig.9) at 2300-2200 cm⁻¹ in 30-40min. While in copolymer, the nitrile peak at 2250 cm⁻¹ and 2280 cm⁻¹ emerged. The peak at 2250 cm⁻¹ was attributed to C≡N conjugated with unsaturated aliphatic chain or aromatic groups, and 2280 cm⁻¹ was attributed to C≡N connected with saturated bond, such as formonitrile or acetonitrile. As seen from the Gram-Schmidt intensity curves, the peak at 2250 cm⁻¹ appeared later. Gram-Schmidt intensity curves in Fig.10 showed that the nitrile peak at 2250cm⁻¹ and 2280cm⁻¹ emerged at 285 °C, peaked at 355 °C and 450 °C, respectively, and ended at about 600 °C.

Intra-molecule imidization mainly resulted in glutarimide [36,38] and ramification, followed by imide emit; inter-

molecule imidization led to crosslinking, followed by imide degradating into nitriles, then nitriles emitting. From these results, it's obvious that in copolymer, PAM segment adjacent to NVP intended to form H-bond and kept stable to higher temperature nearly before local chain scission took place at 350 ^{o}C. At the same time, NVP promoted remote segment or inter-molecule crosslinking and thus postponed initial backbone breakdown.

Pyrrolidone Analysis

Pyrolidone mainly came from NVP side group splitting at about 400 ^{o}C, which is similar to NVP homopolymer degradation. [39] As previously mentioned, the peak at 1660 cm^{-1} was attributed to acrylamide and pyrrolidone, while 1626 cm^{-1} was attributed to acrylamide. To confirm the correlation between the two peaks and then ensure the existence of acrylamide, synchronous 2D IR maps of PAM and copolymer were shown in Fig.11. Strong correlations are shown between the low-wavenumber sides of IR absorptions at (1625.9 cm^{-1}, 1660.4 cm^{-1}), indicating that acrylamide appeared in this region. To confirm the existence of pyrrolidone, the Gram-Schmidt intensity cures were calculated from Fig.12 by subtracting acrylamide peak and then it came out that the pyrolidone absorbance peak took up 10.8% of the 1660 cm^{-1} absorbance peak area. The trend along with pyrolysis products was a little different from that of NVP homopolymer, [10, 19] indicating that NVP interacted with acrylamide at lower temperature and the interaction kept stable before the main chain breakdown. That is, NVP restrained side group removal until its own side group was removed, which was accounted for the NVP carbonyl developing H-bond with adjacent amide hydrogen.

Copolymer maximum thermal degradation

From DTG curves, the sharp degradation peak at 400 ^{o}C was detected for both PAM and copolymer. To further study the pyrolysis products at this temperature, the IR maps around 35 min were displayed in Fig.14. Carbon dioxide, ketone, amide, imide and ammonia were detected in both maps, while for copolymer, a small peak for nitrile was also seen, and relative intensity for common pyrolysis products was different. Saturated C-H peak at 2900 cm^{-1} accompanied with nitriles, pyrrolidone and imide groups, while ketone absorption peak was moderate compared with PAM. Ammonia, imide, amide and carbon dioxide which principally appeared at lower temperature, emitted at 400 ^{o}C accompanying pyrrolidone, verifying that NVP deferred side chain breakdown by inter and intra-molecule H-bond with amide group, especially inter-molecule H-bond. This can be explained that in PAM, more H in amide surrounded C=O group led to intra-molecule H-bond, while NVP introduced C=O but H and increase the steric hindrance at the same time, resulting in more inter-molecule H-bond or interaction, so that protected neighboring molecule side chain and promoted inter-molecule imidization and postponed initial main chain breakdown.

In conclusion, nitriles was individually detected in copolymer between 350 ^{o}C and 450 ^{o}C, which mainly came from imide in backbone and isolated amide group, indicating that NVP protected surrounding amide group by forming H-bond and promoted the remote side group or inter-molecule crosslinking. Pyrrolidone emitted at 400 ^{o}C, the maximum degradation temperature, accompanied by more low temperature pyrolysis products in copolymer, such as ammonia, imide, amide and carbon dioxide, verifying that NVP stabilized the side group until its own breakdown.

Conclusions

PAM and a series of N-vinylpyrrolidone copolymer with approximate molecule weight were successfully synthesized and their chemical structures were characterized via FTIR and H NMR. The thermal degradation of PAM and copolymers was studied using DSC and coupled TG-FTIR on gaseous pyrolysis products. It was found that NVP played an important role in copolymer stability and degradation: first, large steric hindrance of NVP enhanced the backbone rigidity, thus improved T_gs of copolymers; second, carbonyl of NVP was easier to form H-bond with amide in PAM segment, protecting the adjacent side group at lower temperature; third, NVP promoted the remote side group or inter-molecule crosslinking. As a result, NVP stabilized the PAM side group below 300 ^{o}C, and retarded main chain breakdown until its own breakdown at 400 ^{o}C.

Notes and references

^{a,b,c}College of Polymer Science and Engineering, State Key Laboratory of Polymer Materials Engineering, Sichuan University, Chengdu 610065, China.

email: Guangsu Huang@scu.edu.cn (G.S. Huang), zhengjing@scu.edu.cn (J. Zheng)

1. Khedher N B, David J, Trop I, et al. Imaging findings of breast augmentation with injected hydrophilic polyacrylamide gel: patient reports and literature review[J]. European journal of radiology, 2011, 78(1): 104-111.
2. Hoffman A S. Hydrogels for biomedical applications[J]. Advanced drug delivery reviews, 2002, 54(1): 3-12.
3. DNA adducts[J]. Cancer letters, 2013, 334(1): 5-9.
4. Phillips D H. On the origins and development of the 32P-postlabelling assay for carcinogen–DNA adducts[J]. Cancer letters, 2013, 334(1): 5-9.
5. Underwood A P, Dallman T, Thomson N R, et al. Public health value of next-generation DNA sequencing of enterohemorrhagic Escherichia coli isolates from an outbreak[J]. Journal of clinical microbiology, 2013, 51(1): 232-237.
6. Wang W, Lu J J, Gu C, et al. Performing Isoelectric Focusing and Simultaneous Fractionation of Proteins on A Rotary Valve Followed by Sodium Dodecyl–Polyacrylamide Gel Electrophoresis[J]. Analytical chemistry, 2013, 85(14): 6603-6607.
7. Singh S, Mishra S K, Gupta B D. SPR based fibre optic biosensor for phenolic compounds using immobilization of tyrosinase in polyacrylamide gel[J]. Sensors and Actuators B: Chemical, 2013, 186: 388-395.
8. Ganesh B, Kalpana D, Renganathan N G. Acrylamide based proton conducting polymer gel electrolyte for electric double layer capacitors[J]. Ionics, 2008, 14(4): 339-343.
9. Tang Q, Wu J, Sun H, et al. Superabsorbent conducting hydrogel from poly (acrylamide-aniline) with thermo-sensitivity and release properties[J]. Carbohydrate polymers, 2008, 73(3): 473-481.
10. Loría-Bastarrachea M I, Herrera-Kao W, Cauich-Rodríguez J V, et al. A TG/FTIR study on the thermal degradation of poly (vinyl pyrrolidone)[J]. Journal of thermal analysis and calorimetry, 2011, 104(2): 737-742.

11. Bu-Lin Z, Bing H, Sheng-Li K, et al. A polyacrylamide gel phantom for radiofrequency ablation[J]. International Journal of Hyperthermia, 2008, 24(7): 568-576.

12. Prokop A F, Vaezy S, Noble M L, et al. Polyacrylamide gel as an acoustic coupling medium for focused ultrasound therapy[J]. Ultrasound in medicine & biology, 2003, 29(9): 1351-1358.

13. (a). Zolfaghari R, Katbab A A, Nabavizadeh J, et al. Preparation and characterization of nanocomposite hydrogels based on polyacrylamide for enhanced oil recovery applications[J]. Journal of applied polymer science, 2006, 100(3): 2096-2103. (b). Salehi R, Arsalani N, Davaran S, et al. Synthesis and characterization of thermosensitive and pH-sensitive poly (N-isopropylacrylamide-acrylamide-vinylpyrrolidone) for use in controlled release of naltrexone[J]. Journal of Biomedical Materials Research Part A, 2009, 89(4): 919-928. (c). Dadhaniya P V, Patel M P, Patel R G. Swelling and dye adsorption study of novel superswelling [acrylamide/N-vinylpyrrolidone/3-(2-hydroxyethyl carbamoyl) acrylic acid] hydrogels[J]. Polymer Bulletin, 2006, 57(1): 21-31. (d). Dadhaniya P V, Patel M P, Patel R G. Copper and Nickel Removal from Aqueous Solutions Using New Chelating Poly [Acrylamide/N-vinyl pyrrolidone/3-(2-hydroxyethyl carbamoyl) acrylic acid] Hydrogels[J]. Journal of Macromolecular Science, Part A: Pure and Applied Chemistry, 2007, 44(7): 769-777.

14. Scheirs J, Bigger S W, Then E T H, et al. The application of simultaneous chemiluminescence and thermal analysis for studying the glass transition and oxidative stability of poly (N-vinyl-2-pyrrolidone)[J]. Journal of Polymer Science Part B: Polymer Physics, 1993, 31(3): 287-297.

15. Peniche C, Zaldívar D, Pazos M, et al. Study of the thermal degradation of poly (N-vinyl-2-pyrrolidone) by thermogravimetry–FTIR[J]. Journal of applied polymer science, 1993, 50(3): 485-493.

16. Dong J, Fredericks P M, George G A. Studies of the structure and thermal degradation of poly (vinyl chloride)-poly (N-vinyl-2-pyrrolidone) blends by using Raman and FTIR emission spectroscopy[J]. Polymer degradation and stability, 1997, 58(1): 159-169.

17. Polacco G, Cascone M G, Petarca L, et al. Thermal behaviour of poly (methacrylic acid)/poly (N-vinyl-2-pyrrolidone) complexes[J]. European polymer journal, 2000, 36(12): 2541-2544.]

18. Lau C, Mi Y. A study of blending and complexation of poly (acrylic acid)/poly (vinyl pyrrolidone)[J]. Polymer, 2002, 43(3): 823-829.

19. Bianco G, Soldi M S, Pinheiro E A, et al. Thermal stability of poly (N-vinyl-2-pyrrolidone-co-methacrylic acid) copolymers in inert atmosphere[J]. Polymer degradation and stability, 2003, 80(3): 567-574.

20. Kuo S W, Chang F C. Significant thermal property and hydrogen bonding strength increase in poly (vinylphenol-co-vinylpyrrolidone) copolymer[J]. Polymer, 2003, 44(10): 3021-3030.

21. Biswal D R, Singh R P. Characterisation of carboxymethyl cellulose and polyacrylamide graft copolymer[J]. Carbohydrate Polymers, 2004, 57(4): 379-387.

22. Yang M H. The thermal degradation of polyacrylamide with adsorbed metal ions as stabilizers[J]. Polymer testing, 2000, 19(1): 85-91.

23. Du Y K, Yang P, Mou Z G, et al. Thermal degradation behaviors of PVP coated on platinum nanoparticles[J]. Journal of applied polymer science, 2006, 99(1): 23-26.

24. Moharram M A, Khafagi M G. Thermal behavior of poly (acrylic acid)–poly(vinyl pyrrolidone) and poly (acrylic acid)–metal–poly (vinyl pyrrolidone) complexes[J]. Journal of applied polymer science, 2006, 102(4): 4049-4057.

25. Natkański P, Kuśtrowski P, Białas A, et al. Thermal stability of montmorillonite polyacrylamide and polyacrylate nanocomposites and adsorption of Fe (III) ions[J]. Applied Clay Science, 2013, 75: 153-157.

26. Köhler J. Poly (vinylpyrrolidone)-coated silica: A versatile, polar stationary phase for HPLC[J]. Chromatographia, 1986, 21(10): 573-582.

27. Tóth I, Szépvölgyi J, Jakab E, et al. Thermal degradation of a bentonite-polyacrylamide complex[J]. Thermochimica acta, 1990, 170: 155-166.

28. Belyakova L A, Varvarin A M, Lyashenko D Y, et al. Study of interaction of poly (1-vinyl-2-pyrrolidone) with a surface of highly dispersed amorphous silica[J]. Journal of colloid and interface science, 2003, 264(1): 2-6.

29. Maensiri S, Laokul P, Promarak V. Synthesis and optical properties of nanocrystalline ZnO powders by a simple method using zinc acetate dihydrate and poly (vinyl pyrrolidone)[J]. Journal of crystal growth, 2006, 289(1): 102-106.

30. Hsin Y L, Hwang K C, Yeh C T. Poly (vinylpyrrolidone)-modified graphite carbon nanofibers as promising supports for PtRu catalysts in direct methanol fuel cells[J]. Journal of the American Chemical Society, 2007, 129(32): 9999-10010.

31. Chrissafis K, Paraskevopoulos K M, Papageorgiou G Z, et al. Thermal and dynamic mechanical behavior of bionanocomposites: fumed silica nanoparticles dispersed in poly (vinyl pyrrolidone), chitosan, and poly (vinyl alcohol)[J]. Journal of applied polymer science, 2008, 110(3): 1739-1749.

32. Kitahara Y, Okuyama K, Ozawa K, et al. Thermal degradation of acrylamide from polyacrylamide[J]. Journal of thermal analysis and calorimetry, 2012, 110(1): 423-429.

33. Borodko Y, Habas S E, Koebel M, et al. Probing the interaction of poly (vinylpyrrolidone) with platinum nanocrystals by UV-Raman and FTIR[J]. The Journal of Physical Chemistry B, 2006, 110(46): 23052-23059.

34. Zhang R, Hu Y, Li B, et al. Studies on the preparation and structure of polyacrylamide/α-zirconium phosphate nanocomposites[J]. Journal of materials science, 2007, 42(14): 5641-5646.

35. Marini A, Berbenni V, Capsoni D, Riccardi R, Zerlia T. Factors affecting the spectral response in a TG/FTIR experiments. Appl Spec 1994;48:1468–71

36. Van Dyke J D, Kasperski K L. Thermogravimetric study of polyacrylamide with evolved gas analysis[J]. Journal of Polymer Science Part A: Polymer Chemistry, 1993, 31(7): 1807-1823.

37. Chalapathi VV, Ramiah KV, Curr Sci 1968; 16: 453.

38. Leung W M, Axelson D E, Van Dyke J D. Thermal degradation of polyacrylamide and poly (acrylamide‐co‐acrylate)[J]. Journal of Polymer Science Part A: Polymer Chemistry, 1987, 25(7): 1825-1846.

39. Peniche C, Zaldívar D, Pazos M, et al. Study of the thermal degradation of poly (N-vinyl-2-pyrrolidone) by thermogravimetry–FTIR[J]. Journal of applied polymer science, 1993, 50(3): 485-493.
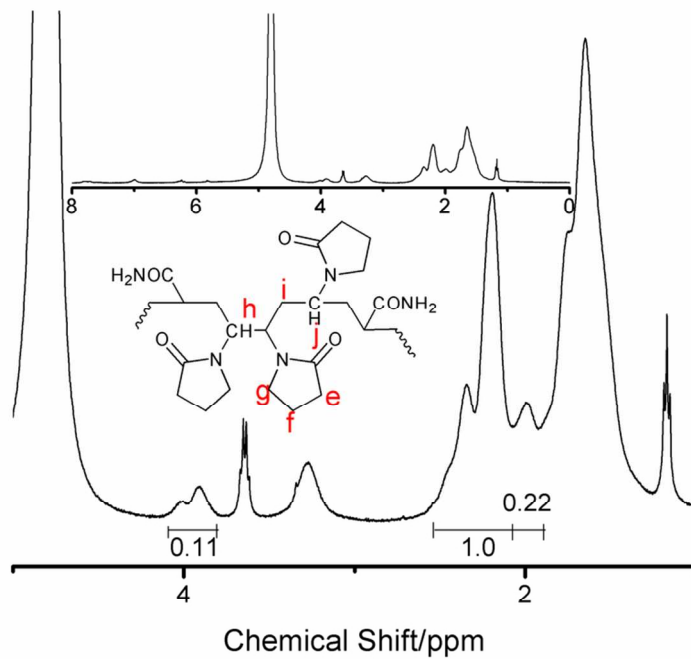
40. Schild H G. Thermal degradation of PNIPAAM: TGA–FTIR analysis[J]. Journal of Polymer Science Part A: Polymer Chemistry, 1996, 34(11): 2259-2262.
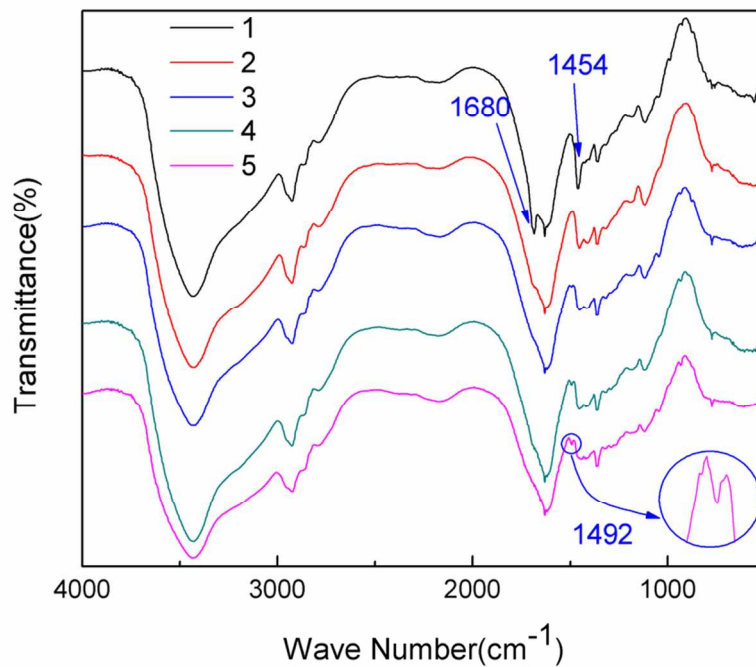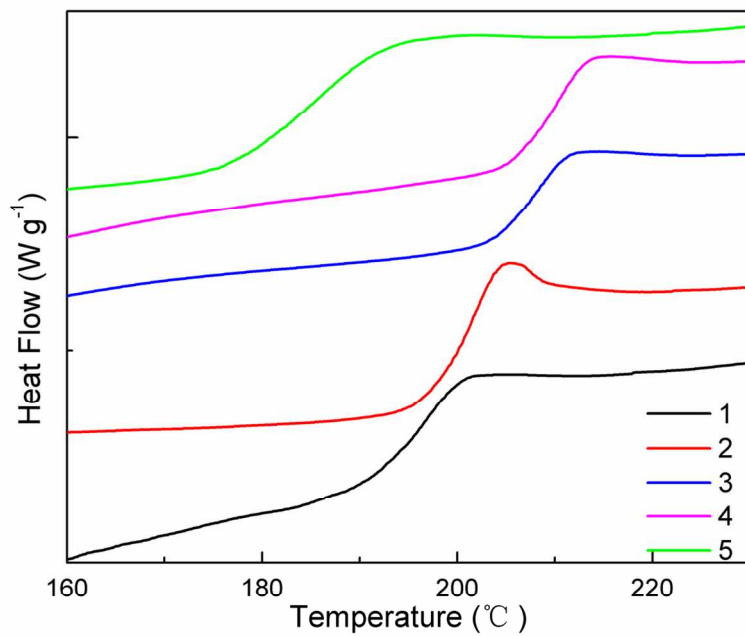
Stacked FTIR spectrum of (a): (1) PAM; (2) P(AM-NVP-1%); (3) P(AM-NVP-5%); (4) P(AM-NVP-10%); (5) P(AM-NVP-15%) and (b): PAM and P(AM-NVP-15%).
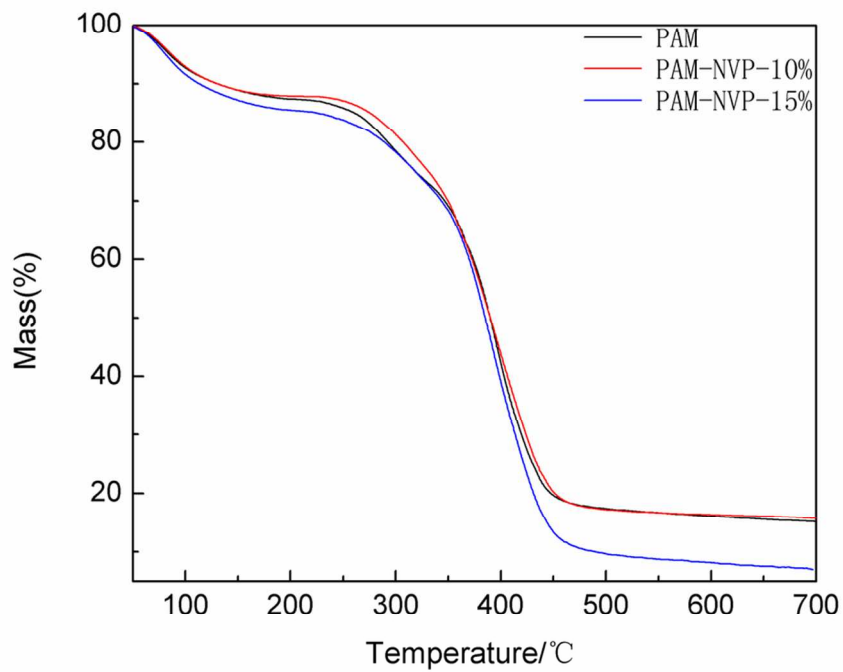46x35mm (600 x 600 DPI)
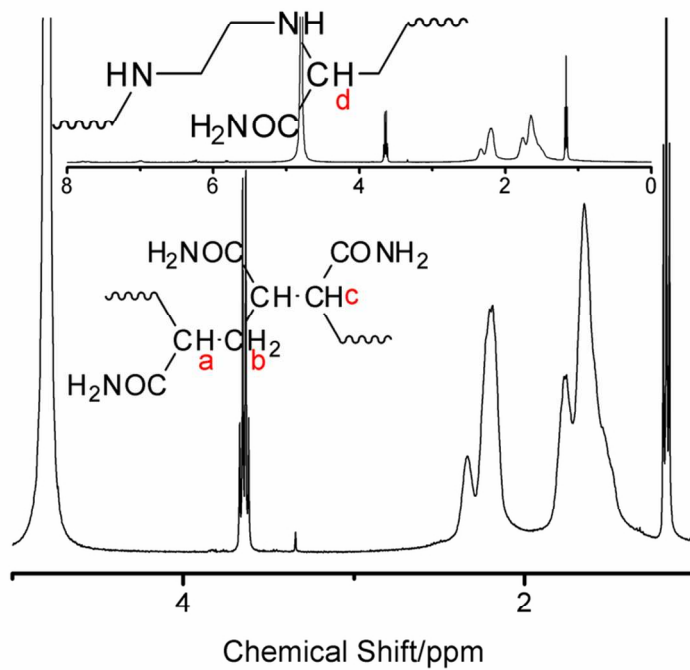
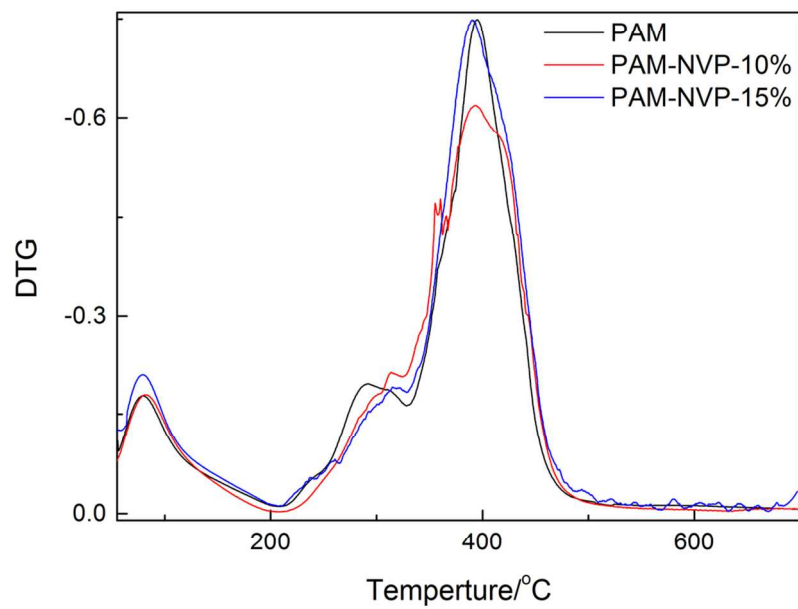H NMR of (a) PAM and (b) copolymer.
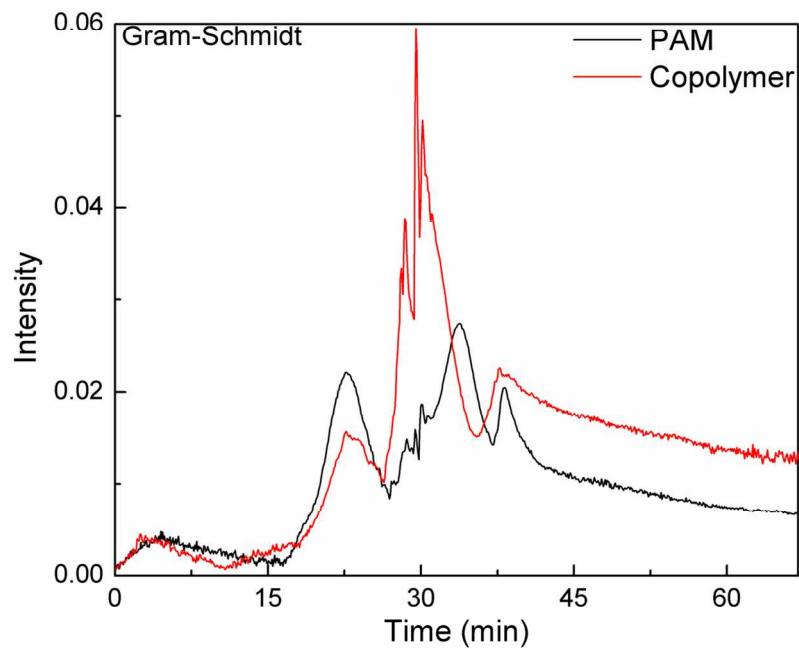46x35mm (600 x 600 DPI)

46x35mm (600 x 600 DPI)

DSC curves of (1) PAM; (2) P(AM-NVP-1%); (3) P(AM-NVP-5%); (4) P(AM-NVP-10%); (5) P(AM-NVP-15%).
61x47mm (600 x 600 DPI)

TGA curves of PAM and copolymer.
46x35mm (600 x 600 DPI)

DTG curves of PAM and copolymers.
56x40mm (600 x 600 DPI)

The total Gram-Schmidt intensity of PAM and copolymer.
61x47mm (600 x 600 DPI)
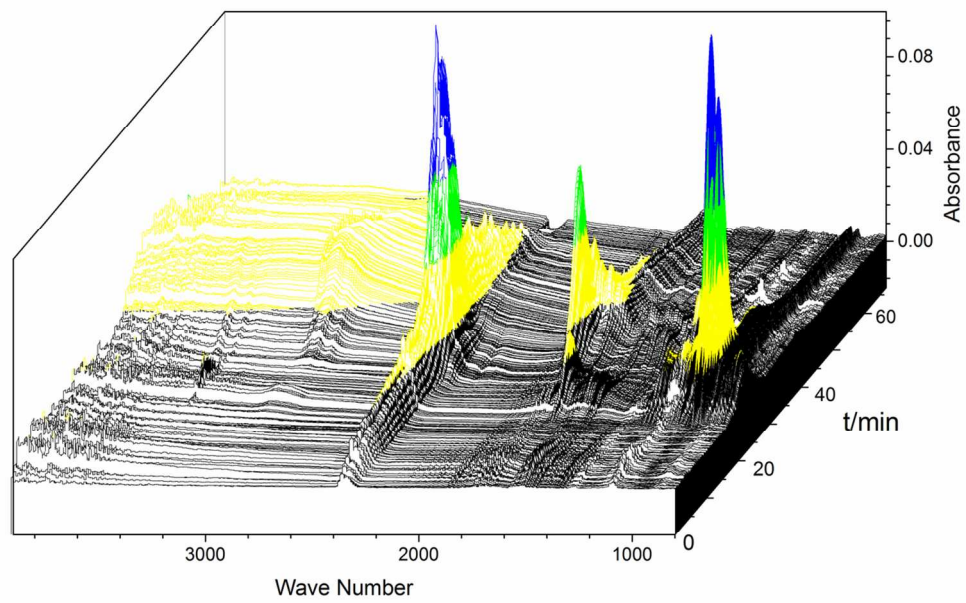
The real-time tracking infrared spectrums of (a) PAM and (b) copolymer.
56x39mm (600 x 600 DPI)
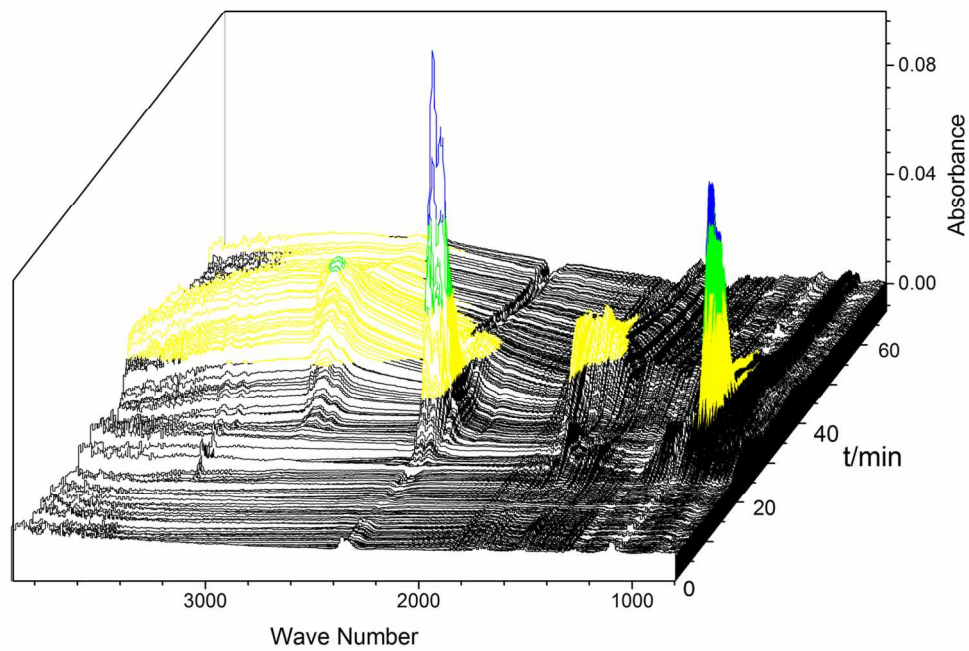
61x47mm (600 x 600 DPI)
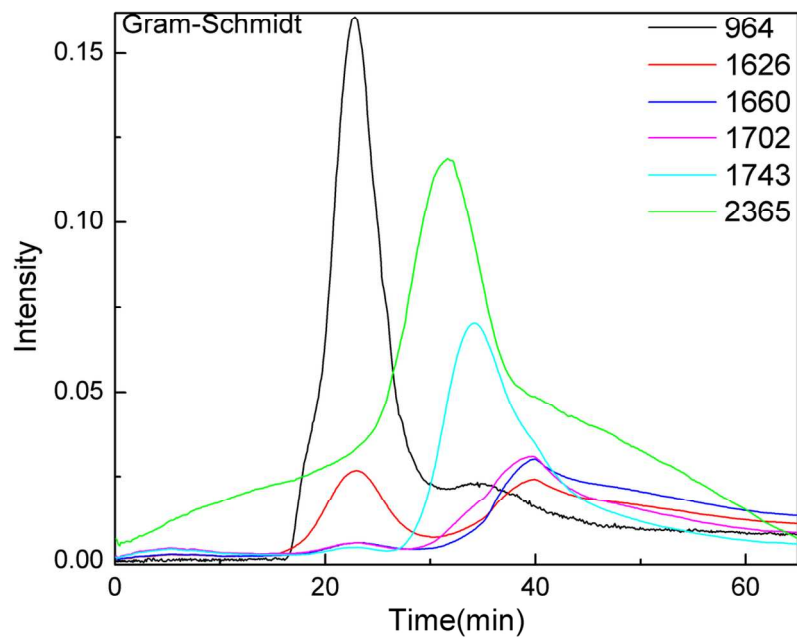
Gram-Schmidt curves of main pyrolysis products for (a) PAM and (b) copolymer.
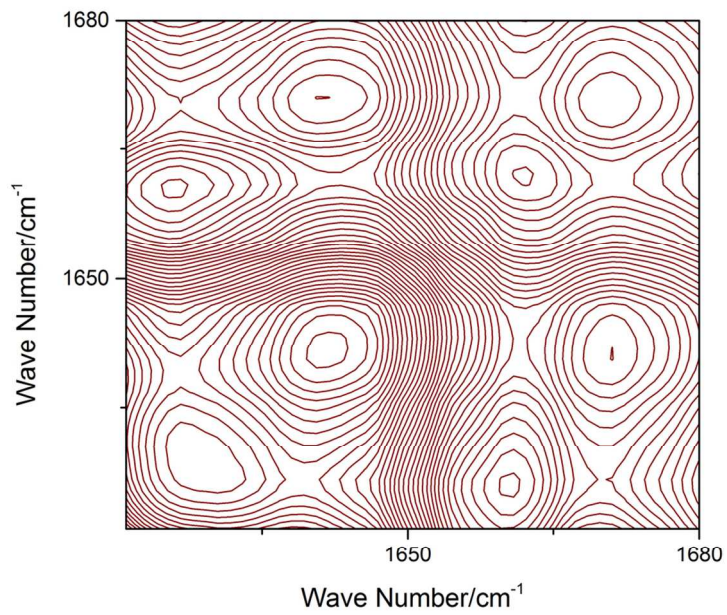61x47mm (600 x 600 DPI)
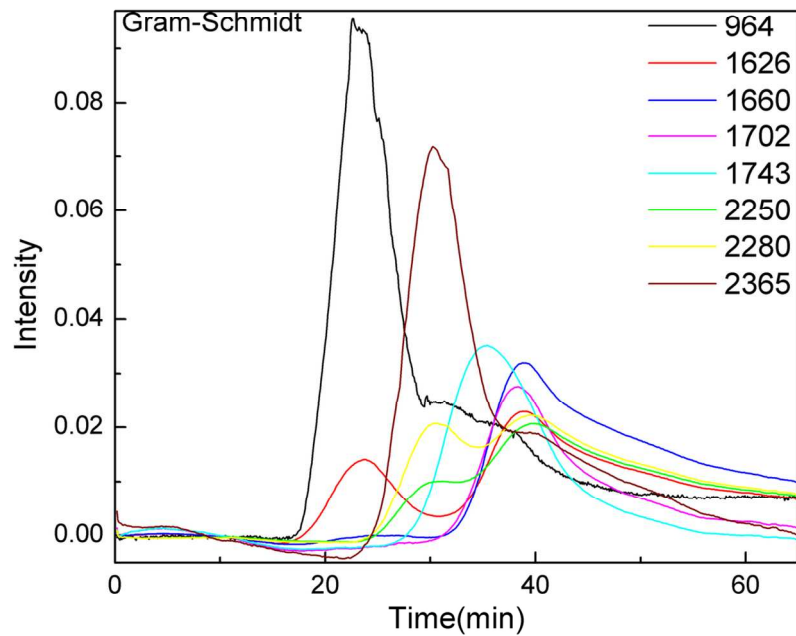
61x47mm (600 x 600 DPI)
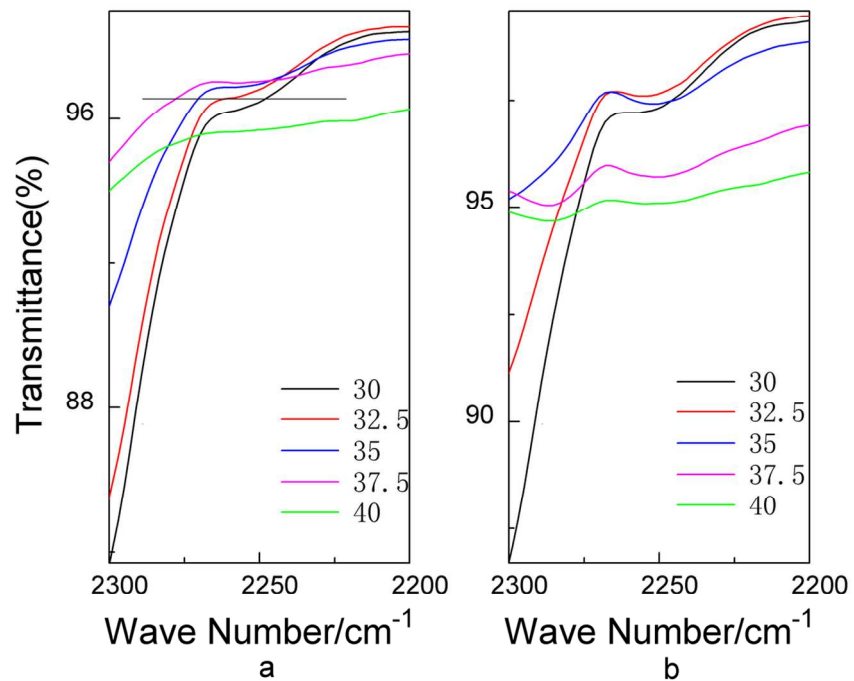
Expanded FTIR spectrum of evolved gas between 350℃ and 450℃ for (a). PAM and (b). copolymer.
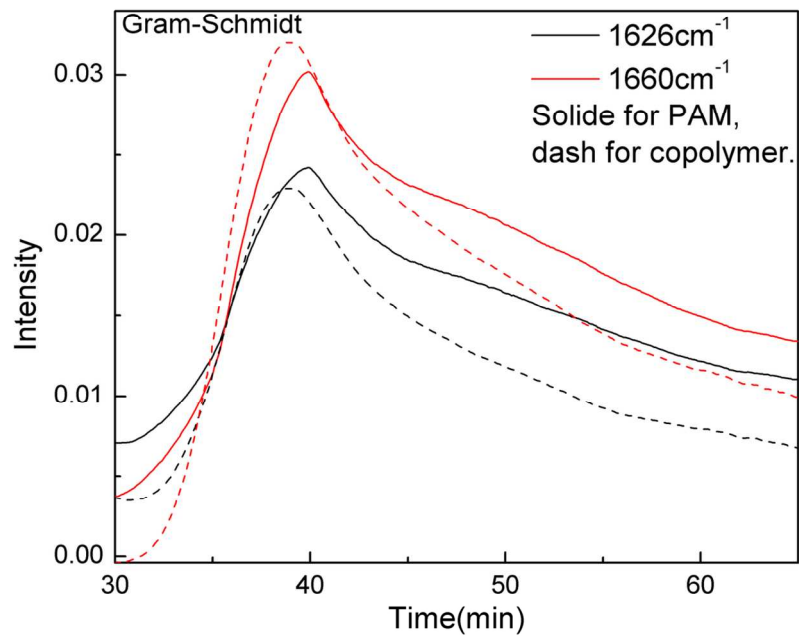61x47mm (600 x 600 DPI)
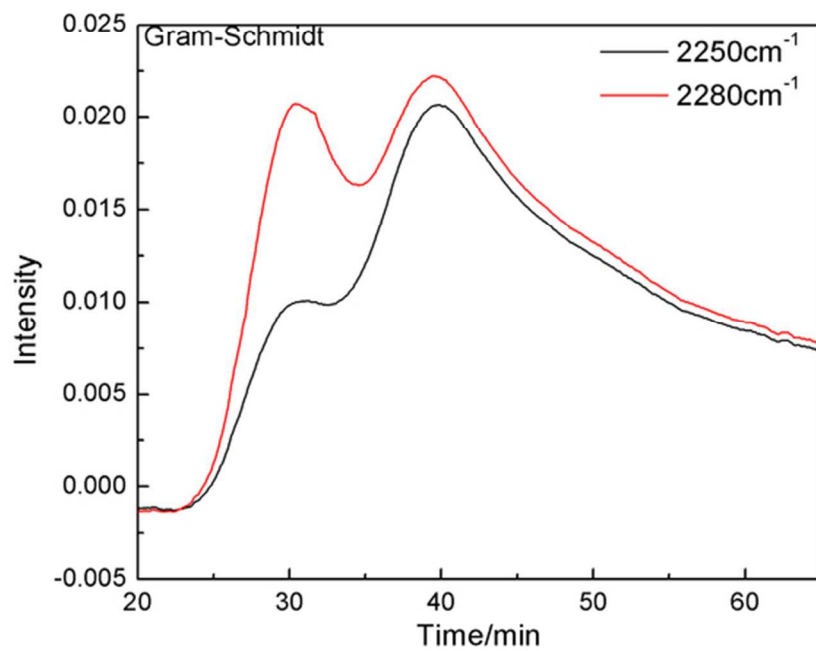
Gram-Schmidt curves of copolymer pyrolysis products: nitriles.
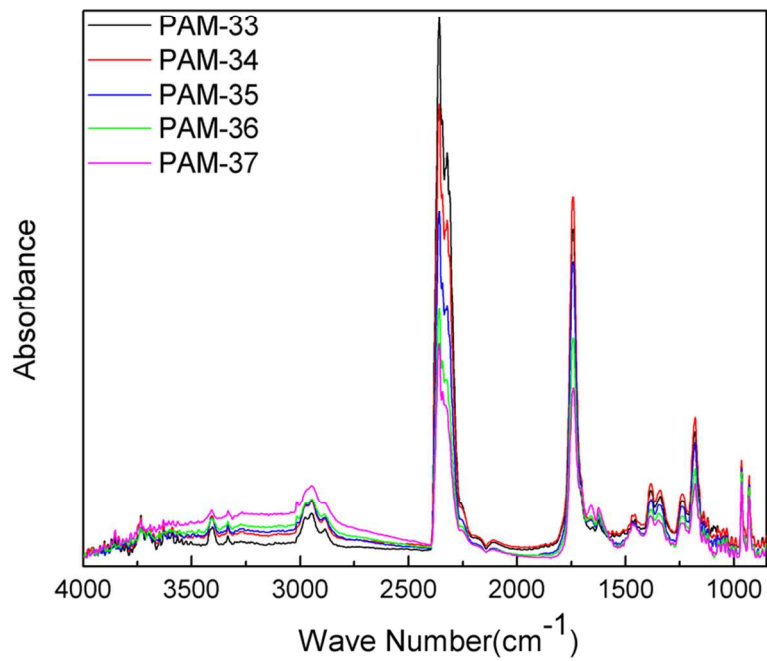57x44mm (300 x 300 DPI)
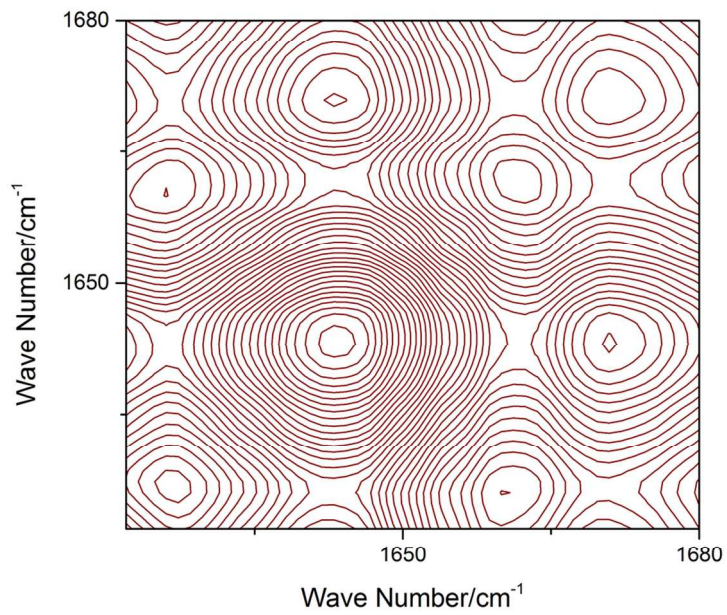
Synchronous 2D IR maps of (a) PAM and (b) copolymer in 35~45min.
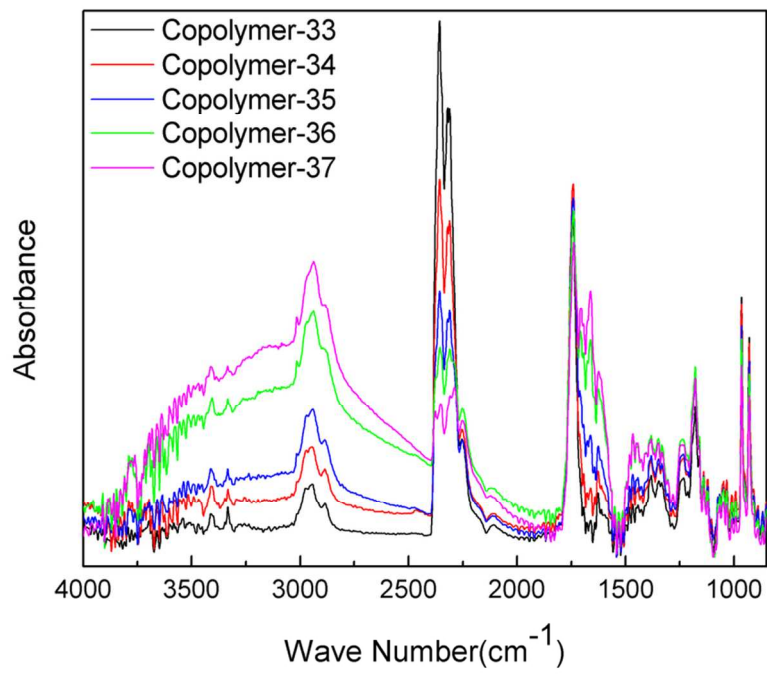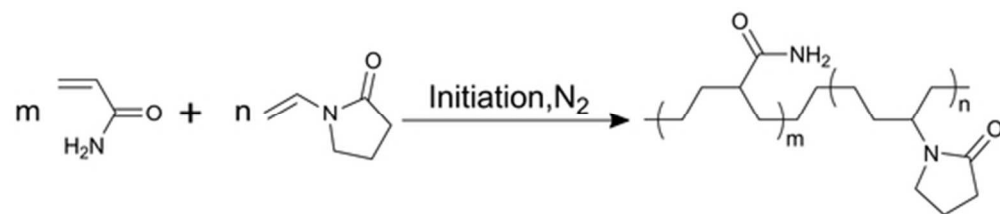56x40mm (600 x 600 DPI)

56x40mm (600 x 600 DPI)

Gram-Schmidt curves of amide and pyrrolidone.
61x47mm (600 x 600 DPI)

46x35mm (600 x 600 DPI)

46x35mm (600 x 600 DPI)

24x5mm (600 x 600 DPI)

Table 1. Intrinsic Viscosity of all specimens.

NVP Content (mol%)	0	1	5	10	15
Intrinsic Viscosity $(mL\ g^{-1})$	1008.43	985.23	1021.48	994.92	1036.51

Table 2. Thermogravimetric analysis of PAM and copolymer.

Specimens	First stage, content (%)	Second stage, content (%)	Third stage, content (%)
PAM	50-207, 12.65	207-329, 14.00	329-535, 56.46
PAM-NVP-10%	50-209, 12.11	209-330, 12.61	330-564, 58.71
PAM-NVP-15%	50-202, 14.53	202-327, 12.02	327-564, 64.89